Active tectonics of plate boundary zones and the continuity of plate boundary deformation from Asia to North America

Jeffrey T. Freymueller

Geophysical Institute, University of Alaska Fairbanks, Fairbanks, AK 99775, USA

Pervasive fragmentation of continental lithosphere at plate boundaries is the rule, not the exception. However, over most of the plate boundary zones of Asia and western North America, crustal motions observed by geodesy can be described well by models that use a number of rigid plates or blocks, bounded by faults that are presumed to cut the entire lithosphere. Only a few areas, mostly in the Tibetan Plateau, may be exceptions to this rule because they display a more continuum-like deformation pattern. This might result from deformation that is distributed broadly at depth, even if it is mainly localized at the surface. The lithosphere of deforming Asia and North America is fragmented into several large rigid or very slowly straining regions, most likely small plates within the plate boundary zone. Most of these small plates move slowly, making the definition of the plates and their boundaries sometimes controversial. The plate boundary zones of Asia and North America are connected as part of a broad band of distributed deformation that marks the entire northern Pacific Rim. Distributed deformation is continuous or nearly so from Baja California around the north Pacific to Tibet, and beyond. Study of plate boundary zones is complicated by temporal variations in deformation. Despite the time dependence implied by postseismic deformation models, the concept of an interseismic period dominated by steady deformation with time appears to remain valid. Development of an earthquake cycle model that explains both pre- and post-earthquake observations remains an area of active research. In addition, there is some evidence for changes in fault slip rates over time, particularly when pairs of faults within a small area show coupled behaviour.

Keywords: Active tectonics, elastic deformation, plate motion, space geodesy.

Introduction – plate boundary zones

ACCORDING to classic plate tectonic theory as developed in the 1960s, Earth's crust is divided into a set of plates that move relative to each other, each plate is rigid, and all deformation occurs within narrow zones at the plate boundaries. However, it was recognized from an early stage that seismicity and active tectonics could be distributed across large areas, especially in the continental crust. These broad areas of distributed continental tectonic deformation are termed *plate boundary zones*, reflecting the fact that each plate boundary zone spans a boundary between plates and the cumulative deformation across it corresponds to the total relative plate motion. Outside of plate boundary zones, the approximation of rigid plates moving at a steady rate over millions of years is quite good. While there is evidence for non-zero internal deformation of the plate interiors, that rate of deformation is a small fraction of the rate of plate motion[1,2].

Early plate models explained the most important tectonic features on the planet using a small number of plates (10–20). Today the number of major and minor plates is reckoned to be several times larger. For example, the PB2002 model[3] uses 52 plates, including many small plates and microplates as well as areas of distributed deformation where the idea of plate tectonics, if it applies, requires the 'plates' to be very small. Detailed models of broad deforming areas such as western North America suggest that plate tectonic-like models may apply even down to the scale of blocks with dimensions of tens of kilometers[4].

Two important sets of questions related to the scale of plate-like behaviour and the extent of plate boundary zones will be addressed in this paper, using examples from the plate boundary zones of North America and Asia:

(1) What is the lower scale limit for 'plate-like' behaviour? All deforming zones consist of a network of active faults, some of which may be very close together. At what point can the deformation resulting from these faults be usefully described as plate-like? Are there regions on the Earth where deformation is distributed broadly enough that a plate-like description cannot describe the motions adequately?

(2) At what scale do temporal variations in deformation associated with the rheology of fault zones and the lithosphere and asthenosphere become important factors in describing active tectonic movements? How much does the non-elastic behaviour of the Earth affect estimates of

e-mail: jeff.freymueller@gi.alaska.edu

steady tectonic motions? There is evidence for variations in fault slip rates with time, sometimes involving paired structures that alternate in activity. Over what scale do slip rate variations affect a model of tectonic motions?

The answers to these questions require us to think about how our ability to measure and to model something can be separated from what is actually happening in the Earth. The second question, if we can answer it, probes at the underlying dynamics that produce the approximately steady kinematic behaviour that we observe.

Defining and modeling rigid plate motion through space geodesy

The motion of a rigid plate on the surface of a sphere can be described by a rotation about an axis passing through the geocentre, described by a single angular velocity vector. Models of plate motions consist of angular velocities of plates relative to some reference frame, or angular velocities of relative plate motions. Given the angular velocity of a plate, the horizontal velocity v of a geodetic site fixed to the crust is the vector cross product of the plate angular velocity ω and the geocentric site position $v = \omega \times r$.

Although there are three components to the vector v, when v is expressed in the local east-north-up coordinate system defined at the site, the up component of v is always zero. The simple plate tectonic model predicts that all motion is horizontal, and this approximation is good for the plate interiors, leaving aside isostatic effects. Even close to plate boundaries, the approximation of no-net-vertical tectonic motion is fairly good except at convergent boundaries where vertical motions can be significant.

The plate angular velocities ω and the site velocities v are given in a specific reference frame. The reference frame specifies the geocentre and direction of the coordinate axes, and defines zero velocity and zero rotation. In geodetic terms, the scale and scale rate are defined as well, through the speed of light and the Earth's gravity field. A reference frame may be fixed to a particular plate or defined based on some global criterion. The former is convenient for studying plate boundary deformation, but awkward for global geodesy. In order to distinguish between plate motions and earth rotation variations, the International Terrestrial Reference Frame (ITRF) defines zero rotation using a condition of no-net-rotation of the lithosphere, and today all geodetic solutions use some version of ITRF. The most recent realization of the ITRF is ITRF2008 (http://itrf.ensg.ign.fr/ITRF_solutions/2008/). Plate motions can be estimated by determining the plate angular velocities in ITRF[5,6], or by estimating relative plate angular velocities and geocentre motion directly from a set of geodetic data[2]. The first approach provides a set of absolute plate angular velocities, which makes it easy to determine plate motions of any geodetic site relative to any plate. The second approach yields relative plate angular velocities, which can be compared directly with geological indicators of relative plate motion such as spreading rates at mid-ocean ridges or transform fault azimuths[1].

Argus *et al.*[2] showed that while plate motions over the last few decades are very similar to geologic estimates of plate motions over the last ~3 million years, for most plate pairs the differences between geodetic and geologic estimates of plate motions are statistically significant. This implies that changes in plate motions of a few to several per cent have occurred over the last three million years, most notably the reduction in angular speed of the Nazca plate relative to South America[7].

Outside of known regions of tectonic activity the plate interiors are rigid to a level comparable to the measurement precision of GPS[2,8]. Calais *et al.*[8], analysed internal deformation of the eastern part of the North American plate, and found a weighted RMS residual horizontal velocity of 0.7 mm/yr. However, horizontal residuals showed a systematic spatial pattern, interpreted to be the result of glacial isostatic adjustment (GIA). Horizontal deformation from GIA complicates the determination of the angular velocity of the plate itself, so Sella *et al.*[9] used a set of 124 sites selected to minimize the effects of GIA and used these sites to determine an updated estimate of the North American plate. The unweighted rms residuals for these sites were 0.6 mm/yr, consistent with the estimated precision of the measurements. Bounds on plate non-rigidity are similar for the interiors of other large, well-studied plates[2,6]. The Indian plate may be an exception to this rule, most likely due to forces resisting the India–Eurasia collision. Banerjee *et al.*[10] found evidence for north–south contraction across the Indian subcontinent, which could reflect 2 ± 1 mm/yr of shortening across central India.

Elastic deformation and the difference between instantaneous geodetic motions and long-term geologic motions

Geologic data for relative plate motions, or at a smaller scale for slip on faults, reflect long-term motions and permanent deformation of the crust. As mentioned in the previous section, instantaneous geodetic estimates of the motions of sites in plate interiors agree with long-term geologic estimates of plate motions to within a few per cent, but the same is not true in the vicinity of active faults. Close to active faults, geodetic data measure a combination of the long-term motions and elastic deformation that results from variations in slip on the faults with depth. Most of the time the shallow part of a fault does not slip because it is locked by friction, but when deviatoric stresses are large enough to overcome friction,

the fault suddenly slips a large amount (an earthquake) to relieve the accumulated stresses[11]. This cycle of stress accumulation and release results in a cycle of elastic deformation of the Earth surrounding the fault.

The basic concept of the 'earthquake cycle' goes back to Reid's elastic rebound hypothesis, in which he proposed that the strain accumulation pattern between earthquakes would be opposite to the strain release pattern during the earthquakes[12]. The net result of one full cycle of accumulation and release is an approximately block-like offset along with fault, with no strain off the fault – much like what would be observed by geologists studying long-term offsets (Figure 1). In reality, successive large earthquakes on a fault are never identical, but averaged over many earthquake cycles the displacements measured from geodesy and geology would be approximately the same everywhere. In elastic earthquake cycle models, the time period between earthquakes is termed the interseismic phase, and the accumulation of stress (and thus deformation) is linear with time. Although the Earth is not purely elastic and there is unambiguous observational evidence for transient postseismic deformation following earthquakes, the observed deformation prior to large earth quakes is generally observed to be linear with time within

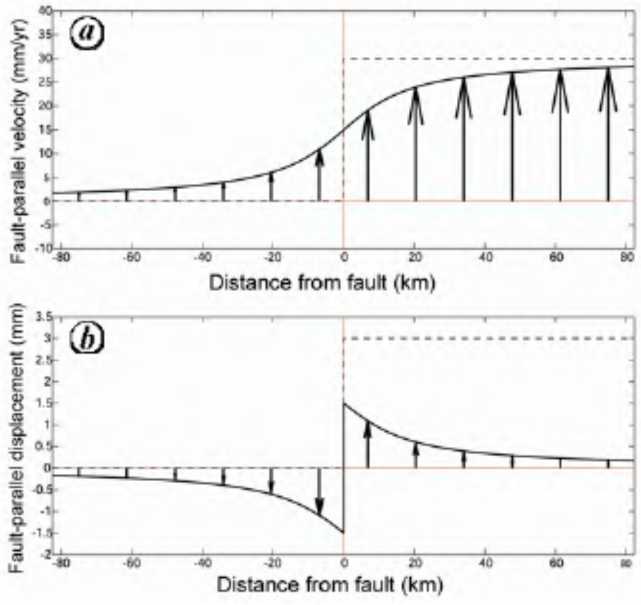

Figure 1. Velocities and coseismic displacements expected from a simple elastic earthquake cycle model. The fault in this model is an infinitely long strike-slip fault (left-lateral) with a slip rate of 30 mm/yr that has an earthquake after 100 years with 3 m slip. During the interseismic period, the fault is locked from the surface to 15 km depth and slipping steadily below that. The interseismic deformation pattern (***a***) is shown by the arrows and solid line, relative to the far field on the left side of the fault. Compared to the uniform block motion that would result if the fault slipped uniformly at all depths (dashed line), the elastic response of the earth spreads the fault shear over a broad area. The coseismic displacement (***b***) is anti-symmetric about the fault, with maximum displacement at the fault (each side moves by half the coseismic slip, in opposite directions). The sum of 100 years of interseismic deformation plus the coseismic displacement is a uniform block motion at the long-term slip rate, shown by the dotted line.

measurement precision and the concept of 'interseismic deformation' remains useful.

The distribution of slip on a fault with depth is of critical importance to the understanding of how geodetic observations relate to long-term fault slip. Large earthquakes within the continental crust rupture only a limited depth range, from at or near the surface to a lower limit that is usually no deeper than 10–20 km. The deeper parts of the fault tend to creep or shear steadily. We define the *slip deficit* as the difference between the slip occurring on a part of the fault and the slip expected based on the long-term slip rate. If a part of a fault is creeping steadily at the long-term slip rate, it has a slip deficit of zero. This leads to a model in which the deeper part of the fault zone creeps continuously at the long-term fault slip rate (no slip deficit), whereas the shallow part of the fault zone remains stuck by friction except in earthquakes (slip deficit accumulates at the long-term slip rate)[13,14]. During the interseismic period, geodetic observations record a combination of the long-term fault motion and elastic deformation that results from the slip deficit on the shallow part of the fault that is frictionally locked.

Numerical models for the interseismic period follow directly from the assumptions of the earthquake cycle model[13,14]. Purely elastic models are typically used. The elastic strain that results is proportional to the slip deficit and its spatial pattern depends on the fault geometry and the depth to which the fault is locked. The elastic deformation can be computed using elastic dislocation theory. The deformation observed geodetically is the superposition of steady fault slip at all depths (termed block motion) and backwards slip on the locked part of the fault (backslip) to represent the slip deficit. The backslip is a mathematical construct, one component of the linear superposition; the fault does not actually slip backwards.

In the two-dimensional case of an infinitely long strike-slip fault, the equations describing the elastic dislocation model are very simple. The velocity of a site located a distance x from the fault $V = (s/\pi) \times \arctan(x/d)$, where s is the average slip rate, and d is the locking depth[13] (Figure 1). This simple function represents the sum of the two parts of the superposition mentioned above, expressed in a frame in which the velocity is zero at the fault ($x = 0$). When the locking depth is shallow, the elastic strain is concentrated close to the fault, and when it is deep the strain is distributed over a larger region. The locking depth provides the appropriate length scale for the extent of the off-fault deformation. For example, 50% of the elastic deformation is found within the region less than one locking depth from the fault, and 90% of the elastic deformation occurs within ~6.3 locking depths from the fault. For the common fault locking depths in the range of 10–15 km, this means 90% of the elastic deformation occurs within the region within 65–95 km of the fault trace. Conversely, this means that

nearly 10% of the elastic signal will be found at distances more than 100 km away from the fault. The simple model shown here assumes an abrupt transition from locked to creeping at the locking depth, whereas a gradual transition with depth may be more realistic. A gradual transition from locked to creeping can be constructed by a superposition of multiple dislocations, where slip becomes a function of depth. In most cases, a model with a continuous transition from locked to creeping predicts very similar surface deformation to a model with an abrupt transition from locked to creeping, so the simpler model is generally used. However, these two cases can predict very different stresses at depth, and singularities at depth are avoided when the slip is a smooth and continuous function of depth. Further research into slow and transient slip (see section on 'temporal variations') may shed more light into the downdip locked to creeping transition and lead to models that produce more realistic stress distributions at depth.

The elastic dislocation approach has been extended to three dimensions using elastic block modeling[15,16], which blends the description of plate motions in terms of angular velocities with an elastic interseismic model. The model domain is broken up into a set of rigid blocks or microplates, bounded by active faults. The velocity of a GPS site is the sum of the rotation of the block it lies on (described by the block angular velocity) and the elastic deformation caused by the slip deficit on all faults in the model. The elastic block model enforces self-consistency of block motions, fault slip rates, and elastic deformation, because the fault slip rates are computed from the block angular velocities and the elastic deformation is computed using dislocation theory from the fault slip rates and assumed fault locking depths. Thus the only estimated parameters in an elastic block model are the block angular velocities, unless the fault locking depths or other geometric parameters are explicitly optimized as well. This approach has been successful in describing deformation in many parts of the world and has sometimes been combined with an assumption of uniform strain for some blocks rather than rigidity[4,15–21].

The elastic deformation component imposes a critical limitation on the resolution of these models. Given the typical range of fault locking depths (10–20 km for most continental faults), the effect of the elastic component is to spread the deformation from a single fault over an area up to tens of kilometers away from the fault (Figure 1). The deformation fields due to two parallel, closely spaced faults will overlap significantly in space and thus will be difficult to separate in an inverse problem. The relevant spatial scale is the fault locking depth, so faults that are a few km apart generally cannot be distinguished from a single fault. Even where faults are separated by roughly twice the locking depth, the deformation field that results from multiple parallel faults will be quite close to a broad linear gradient due to the overlapping elastic effects, and could be modeled in terms of a single fault with a fairly deep locking depth, as has been shown for the northern Coast Ranges of California[22]. This imposes an effective lower limit on the size of crustal blocks that can reasonably be modeled and resolved in deformation models.

Another approach to describing the deformation of plate boundary zones is a distributed strain model, based on the work of Haines and Holt[23] and refined in many subsequent articles. These models describe deformation in terms of a continuous distribution of strain, but do not attempt to explain the strain in terms of its root causes. Haines and Holt[23] showed that such a model can be parameterized in terms of a spatially varying angular velocity $W(r)$ and that strains, rotations and displacements can be determined uniquely from this function and appropriate boundary conditions. They approximated the continuous function $W(r)$ using spline functions that pass through a set of grid points. The advantage of this kind of model is that it allows geodetic data to be combined with seismic estimates of strain rate from time-averaged earthquake moment tensors or geologic estimates of strain rate from fault slip rates. Such a continuous strain model can provide insight into the dynamics of continental deformation when compared with a stress model based on estimated stresses due to plate boundary forces, basal tractions on the lithosphere, and gravitational potential energy[24,25]. However, it sacrifices some of the capability to predict observed deformation close to fault zones, where elastic block models relate the strain pattern to a physical quantity, the fault locking depth. When deformation is considered on a large scale, this is a minor defect and such models can provide useful constraints on plate boundary dynamics.

Recent work on modeling of plate boundary zones

The plate boundary zones of western North America, and Central and East Asia have received a great deal of study and are the best examples for any discussion of models for plate boundary zones. Distributed deformation in western North America (Figure 2) results from the interaction of the North American, Pacific, and Juan de Fuca plates. The Pacific plate is mostly composed of oceanic crust, but includes continental crust in southern and central California, west of the San Andreas Fault system. The oceanic Juan de Fuca plate is subducting beneath North America at the Cascadia subduction zone. The Pacific plate moves laterally relative to North America both north and south of Cascadia and subducts beneath North America in Alaska and the Aleutian arc. Distributed deformation in Asia spans an enormous area that involves relative motion between the African, Arabian, Indian and Eurasian plates, plus subduction of the Australian, Philippine Sea, and Pacific plates along the eastern edge of the plate boundary zone.

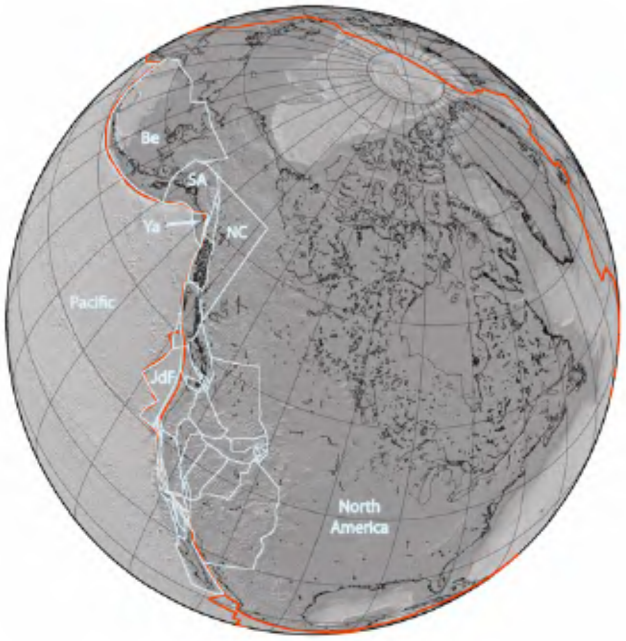

Figure 2. Deforming blocks of North America. Continental crust is in dark gray shading and oceanic crust is in light gray. The classically defined plate boundaries are shown in red, whereas plate and block boundaries based on recent block models are shown in light blue[4,27,37,39]. Smaller plates mentioned in text are indicated by abbreviations: JdF, Juan de Fuca; Ya, Yakutat; NC, Northern Cordillera; SA, Southern Alaska; Be, Bering. The northern and eastern boundaries of the Northern Cordillera (NC) block are uncertain, drawn here as straight lines.

Models for North America

Models for deforming western North America have generally focused on individual regions or parts of the overall plate boundary zone. Numerous models have been developed for the southern part of the boundary zone, which includes the San Andreas Fault system, Basin and Range extensional province, Intermountain seismic belt, and the Cascadia subduction zone. Attempts to construct block models for this region date back to the 1980s and NASA's Crustal Dynamics Project[26]. A few models cover this entire region[27], whereas others focus on parts of this region, for example Meade and Hager[16] for southern California, Payne *et al.*[28] and Puskas and Smith[29] for the western US interior around the Yellowstone Hotspot, and McCaffrey *et al.*[4] for Cascadia. All of these models stop in southern Canada, with the interior of southern British Columbia taken to represent part of the stable North American plate. Some models use only geodetic data, whereas others incorporate fault slip rate estimates from geology and/or time-averaged earthquake moment tensors. Some of the blocks used in these models, particularly the detailed regional models, are as small as 50 km by 100 km in size and the number of blocks can be large. For example, the Pacific Northwest model of McCaffrey *et al.*[4] features 20 blocks to describe the deformation of the overriding plate at the subduction zone.

Models for the northern part of the plate boundary zone, in Alaska and the Northern Cordillera of Canada, are fewer in number. Lahr and Plafker[30] proposed a block model for southern Alaska, based on tectonic patterns and seismicity. The main blocks of this model were the Yakutat block and a rotating Southern Alaska block (termed the Wrangell block by Lahr and Plafker), which is bounded on the north by the Denali Fault. Because few reliable fault slip rates were known at the time, the rates of motion in this model were, in many cases, educated guesses, but for the most part these have proven to be fairly accurate. Fletcher[31] updated this model using rates constrained by GPS data. Mazzotti and Hyndman[32] developed a model for the Northern Cordillera, using the 'orogenic float' hypothesis[33] to explain how deformation propagated a long distance inland from the main plate boundary near the coast. Further refinements of the proposed tectonic models for the Northern Cordillera were based on GPS data and seismicity rate observations[34–36]. Elliott *et al.*[37] developed an elastic block model for southeast Alaska and the Northern Cordillera, based on a large GPS data set. As in the southern part of the boundary zone, additional models have been developed for smaller pieces of the area. Notably, Mazzotti *et al.*[38] analysed data from the Queen Charlotte Islands, between Vancouver Island and southern Alaska, and found that the region had to be moving relative to North America due to active faulting between the islands and the mainland. Cross and Freymueller[39] showed that GPS data from the Bering Sea region and the Aleutian arc and Alaska Peninsula supported the existence of a Bering plate, which rotates clockwise relative to North America.

Models for the India–Eurasia collision zone

Block models for the India–Eurasia collision zone date back a considerable time, and several pre-dated geodetic data from the region. The majority of published models have focused on the Tibetan Plateau and surrounding regions of China, sometimes including Southeast Asia and the Sunda shelf as well. The block model of Avouac and Tapponnier[40], based on estimated slip rates for the major faults, represented one end member in the array of proposed models, with thin viscous sheet continuum models[41] representing the other end member. These early models have since been superseded as new information from geodesy has become available. More recently, block models based on geological constraints have been developed to describe motions for millions of years into the past, most notably by Replumaz and Tapponnier[42].

Several geodetic-based models focused on parts of the collision zone, such as North China[43] or the Eastern Tibet borderland[44]. Chen *et al.*[45] showed that distributed deformation between the major faults of the Tibetan Plateau was of a similar magnitude to the rates of motion on the

major faults. They developed a deforming block model for Tibet, in which the blocks were bounded by major faults and also were subjected to uniform strain. Models spanning a larger part of the region followed the publication of the first comprehensive velocity field for China and later, improved velocity fields[46–48]. Gan *et al.*[48] also showed that the deformation field in Tibet and the surrounding area could be decomposed into sections that displayed rigid block-like behaviour and a region of 'glacier-like flow' in southeastern Tibet, which gave the impression of a continuous deformation field. Meade[20] and Thatcher[49] independently developed elastic block models for all of China, based on the Zhang *et al.*[47] data set. These models will be discussed in more detail in the next section.

Although a great deal of attention has been focused on the India–Eurasia collision zone and the Tibetan Plateau, distributed deformation in Northeast Asia extends for a long distance away from the collision of India and there has long been debate about whether this deformation is all related to the collision of India or to other factors. Calais *et al.*[50] estimated the extension rate across the Baikal rift and proposed a model for the active tectonics of Mongolia. Heki *et al.*[51] presented geodetic evidence for and a model of the motion of the Amurian plate. Cook *et al.*[52] and Riegel *et al.*[53] proposed models for the motion of the Okhotsk plate, based primarily on seismic focal mechanism data. Apel *et al.*[54] estimated poles of rotation for the Amurian and Okhotsk plates based on GPS data. Calais *et al.*[55] developed a combined geodetic solution covering most of East and Northeast Asia and Vergnolle *et al.*[56] used this solution to evaluate dynamic deformation models. Vergnolle *et al.*[56] concluded that the subduction boundaries of East and Southeast Asia (Pacific, Philippines, and Australian plates) play a significant role in the dynamics of deformation in Asia and that eastward motion of South China and North China results from eastward pull from the subduction margins rather than extrusion driven by India.

The lower scale limit of plate-like behaviour

Continental crust tends to deform over broad areas, involving complex networks of faults[57,58]. It is common for a single transform fault to accommodate all of the relative motion between two oceanic plates, but it is rare to find such a simple system in the continental crust, even where the majority of relative motion may occur on a single main structure. Networks of faults are observed at all scales, from outcrop to plate boundary zone. Detailed geometric models of active faults can be constructed in areas that have been intensively studied. For example, the Southern California Earthquake Center (SCEC) Community Fault Model (SCEC-CFM; http://structure.harvard.edu/cfm/themodel.html) features an inventory of more than 130 active faults and provides a detailed 3D geometric model. The model covers an area of 3.5° by 6° and omits many minor faults and near-surface splays from the major faults in the model. Most intensely deforming areas lack data at this level of detail, but there is little reason to believe that all are fundamentally simpler. What level of geological detail is needed to represent motion and deformation in plate boundary zones as measured geodetically? How are interpretations of such models limited by the level of geological complexity that is adopted in the model?

An appealing distinction would be to divide faults into those that cut the entire lithosphere and those that do not (Figure 3). For faults in the first category, deformation at depth must be similar to deformation at the surface (to first order), and a plate-like deformation model must hold. The main difficulty with this idea is that in many cases we are not sure whether or not any particular fault cuts the entire lithosphere! Unambiguous evidence for or against it will be rare, so in practice we usually must fall back on an empirical approach, in which the faults that are included are based in large part on those that are needed to explain the data. This can introduce a considerable component of ambiguity or subjectivity into block models through the choice of which block boundary faults to include[58].

A careful comparison of the block models of Meade[20] and Thatcher[49] for the Tibetan Plateau and surrounding area illustrates the ambiguities in the fault or block geometry. The two models both use the same data[47], but a different number of blocks (17 versus 11 for Meade and Thatcher respectively), and fit the data to about the same

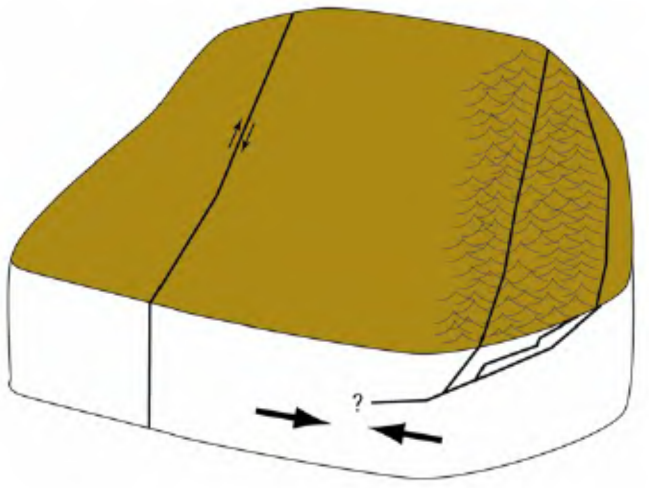

Figure 3. Schematic view of faults that do or do not cut the entire lithosphere. The strike-slip fault at left cuts the entire lithosphere. Deformation is uniform with depth, and thus inherently plate-like. The thrust system at right is comprised of a thin-skinned thrust belt at shallow depth, which transitions to distributed shortening at greater depth. A plate-like approximation may not apply because the deformation at depth is distributed broadly.

level overall (~1.5 mm/yr). The two models are quite similar in most areas, but adopt very different block geometries for the central and southern Tibetan Plateau, and for the southeastern part of the Tibetan plateau, the region between the eastern syntaxis and stable South China. In both of these regions, segments of the block boundaries adopted in the two models are orthogonal to each other, resulting in completely different inferred styles of faulting and fault slip rates. In central Tibet, there is only a single profile of data. Thatcher[49] adopts a single Qiangtang block bounded by the Kunlun and the Karakorum-Jiali fault zones, and found significant residual velocities not explained by the block model. Meade[20] adopted a block boundary that crossed the data profile obliquely, resulting in lower misfit of the data there but depending on a speculative active fault as the block boundary. However, these radical differences are restricted to limited areas.

The relatively similar fit to the data resulting from very different block geometries in certain areas means that we should not put a great deal of confidence in the predictions of the block models for these areas. The areas where the block geometries differ the most are those that show broadly distributed deformation, where perhaps a plate-like model does not apply. Chen *et al.*[45] estimated strain parameters for various regions of the Tibetan Plateau, and found that distributed strain in the regions between major faults resulted in deformation that was comparable in magnitude to the slip on some of the major faults. Gan *et al.*[48] used a more detailed data set and showed significant, relatively uniform strain over broad areas both in central Tibet and southeastern Tibet, exactly the regions where the block models differ most significantly. Elsewhere in the Tibetan Plateau and its borderlands, Gan *et al.*[48] found that a model based on rigid blocks and elastic deformation from the faults that bound them fit the data quite well. Vergnolle *et al.*[56] used a different method to reach a similar conclusion.

It is possible that a plate-like description of the deformation in these complex zones of distributed deformation can be found, and that what appears to be broadly distributed deformation and relatively uniform strain over broad areas simply results from our lack of knowledge of the network of active faults in these areas. Critical information for the development of such a model, however, will need to come from sources other than geodesy. In addition, it remains possible that these regions actually do not deform in a plate-like manner, on any scale that makes sense (given the lithospheric thickness). The Tibetan Plateau has an unusual average crustal rheology due to its exceptionally thick crust, and the viscosity of the thick lower crust must be relatively low compared to typical continental crust. This likely means that some deformation that results in slip on discrete brittle faults in the upper crust is accommodated by bulk deformation of the lower crust rather than by faulting that cuts the entire lithosphere, which is fundamentally not plate-like. Vergnolle *et al.*[56] argued that evidence for continuum or bulk deformation is restricted to a few high elevation/thick crust areas, mainly in Tibet.

Bourne *et al.*[59] proposed an entirely different model for continental deformation and the relationship of surface velocities and fault slip rates. Instead of the plate-like model that is implied in the elastic block and dislocation approach, they argued for a model in which tractions at the base of the lithosphere cause the lower part of the lithosphere to deform in a continuum fashion, such that slip on discrete faults as observed at the surface transitions with depth to continuous deformation at the base of the lithosphere. Although the more plate-like approach is far more commonly used, most authors acknowledge that debate on this topic remains, as surface data can be explained in multiple ways. However, as a description of plate boundary zones in general, most authors support a generally plate-like model over the continuum model based on the concentration of deformation in narrow zones separated by much larger inactive regions[60] or block rotations that are more consistent with edge-driven motion than with basally driven motions[27]. Even where a plate-like model is favored, the mode of deformation must transition to the continuum style at a sufficiently small length scale. At present, that length scale is a matter of dispute, but it is probably comparable to or shorter than the thickness of the lithosphere. As noted above, the exceptionally thick continental crust of the Tibetan Plateau might make parts of Tibet an exception to the general rule.

Continuity of plate boundary deformation from Asia into North America

When all of the work in Asia and North America is considered, there is a continuous or nearly continuous band of distributed deformation that extends from the Gulf of California and Rocky Mountains to the Alpine–Himalayan belt (Figure 4). This region includes the boundary between the North American and Eurasian plates, which has generally been drawn along the Cherskiy Range of eastern Siberia (the pole of Eurasia–North America relative motion lies between the Cherskiy Range and the Arctic Ocean's spreading center). A number of proposed small plates are contained within this band of distributed deformation, including the Bering, Okhotsk, Amurian, and South China plates. Some regions, like the Arctic coast of Alaska and the NE tip of Siberia, are generally considered part of the North American plate, but appear to move slowly relative to North America[61] and thus might lie on another independent block. Here we label this hypothetical block the Chukotka-Arctic Alaska block; it is not clear whether this represents a rigid block or if diffuse deformation and errors in the definition of

North America can explain the observed motion. Deformation processes vary tremendously throughout this vast region, for example the processes driving deformation in the Basin and Range have nothing to do with the opening of the Baikal rift, but distributed deformation is nearly continuous across the entire region. The north Pacific Rim from the west coast of North America through most of Central and East Asia is best described as a collage of small plates, up to 2000–4000 km in size, with deforming boundary zones between them.

We are accustomed, partly by the conventions of our maps, to viewing the deforming zones of Asia and North America as being separate. In reality, this collage of deforming crust spans both sides of the Bering Strait and there is no clear dividing line between a 'North America' domain and a 'Eurasia' domain. Instead, all of the continental margins adjoining the northern Pacific plate are deforming within a broad band. This band of essentially continuous continental deformation could be extended even farther – both westward into the Caucasus and Alpine belt[62], and southward through Central and South America. It may be more accurate to think of the continental crust as deforming everywhere on its plate margins and commonly fragmenting into smaller plates and blocks.

Figure 4. Continuity of distributed deformation around the North Pacific from Asia to North America. The thick red lines show the classically defined plate boundaries, and black lines the small plate or block boundaries as defined by a variety of studies[4,27,37,39,54,93]. Thin red lines show major fault zones in and around the Tibetan plateau[94,95]. Major plates are named, and smaller plates are labeled with abbreviations: Be, Bering; CA, Chukotka-Arctic Alaska (hypothesized); Ok, Okhotsk; Am, Amurian; SC, South China; Su, Sunda.

The rates of deformation or relative plate/block motions are quite low over much of the area described above. For example, the motions of the Amurian and Okhotsk plates relative to Eurasia are only a few millimetre per year, and the motion of the Bering plate relative to North America or Eurasia is of a similar magnitude. In fact, the motion of Eurasia relative to North America along their on-land boundary would be only a few millimetre per year because of the proximity of the pole of relative motion. These rates of motion are small enough that the existence of some of these plates remains disputed. For example, different authors have drawn different boundaries for the Amurian plate, reflecting the presence of distributed deformation within north China[43], and the existence of the Okhotsk plate has been debated (in any case, being mostly underwater, measurement of its motion using GPS is difficult). Kogan and Steblov[63] argued that GPS surveys on Sakhalin Island, which should be on the Amurian–Okhotsk plate boundary, are difficult to reconcile with the estimated relative motion of the two plates. Given the very low deformation rates and uneven sampling of geodetic data at present, it is difficult to distinguish between rigid plates and slow, broadly deforming deformation zones.

Vergnolle *et al.*[56] showed that the observed deformation in Asia requires a model with combination of buoyancy and boundary forces and lateral variations in strength of the lithosphere; elimination of any one of these elements caused a significant increase in the misfit of model predictions to the GPS observations. The preferred model of Vergnolle *et al.*[56] features a number of important elements that match the observations. Their model features broad regions of low strain rate, possibly corresponding to rigid blocks, separated by zones of higher strain that correspond to zones of weakness. They argued that zones of truly continuum-like deformation in Asia are restricted to some of the areas of high topography, mainly on the Tibetan Plateau. Everywhere else, a model of rigid blocks would describe the observed deformation well.

The situation in North America is similar to that of Asia, in terms of the continuity of deforming regions. Elliott *et al.*[37] showed that the crust of the southeast Alaska coast is mobile, moving northward relative to North America. A similar inference, with less specificity, was made by Mazzotti *et al.*[38] based on data from the Queen Charlotte Islands and one site in southeast Alaska. Leonard *et al.*[36] showed that seismic moment tensors and seismicity further support this model. In the block model of Elliott *et al.*[37], the pole of rotation for their Northern Cordillera block relative to North America is located near Vancouver Island. As a result, site motions relative to North America should become very slow close to the pole. Due to the slow motion and sparse data in that part of Canada, Elliott *et al.*[37] were not able to identify the southern boundary of this block and thus the southern boundary of the northern zone of deformation. It is

commonly assumed that southern British Columbia and Vancouver Island are a part of stable North America. McCaffrey *et al.*[4] suggested that both of these regions move relative to North America and the results of Elliott *et al.*[37] support this conclusion, given that the coastal regions both north and south of it are moving northward relative to North America.

Temporal variations

Thus far in this paper, I have made the (implicit) assumption that motions are steady in time, and thus the movements we observe today with GPS should agree with movements measured over geologic time. This uniformitarian assumption is supported by the results for global plate motions, but there are four ways in which it could break down on smaller spatial scales. The first is that short-term, transient slip events have been observed on faults, such as slow slip events (or episodic tremor and slip events)[64,65]. The second is that transient postseismic deformation is observed following large earthquakes and can persist with significant magnitudes for years to decades (and maybe centuries) following a large earthquake. Third, fault slip rates may change over time, either through a slow evolution process or by more abrupt changes involving changes in slip rate of multiple faults. Finally, non-tectonic effects such as GIA, hydrologic surface loading, or deformation due to active volcanism can influence geodetic velocities. This last topic will not be discussed here, except to note that these possibilities need to be considered carefully in every deforming zone.

Slow slip events

Any slip on a fault will cause deformation in the Earth around it, due to the same elastic behaviour discussed before. From this perspective, the only difference between the slip in an earthquake and slip in fault creep is the rate and duration of motion. Slow slip events causing significant deformation have been observed mainly at subduction zones[65]. As with the displacements due to earthquakes, displacements due to slow slip events must be recognized in the time series of positions before site velocities are computed and used in modeling of interseismic deformation. Displacements in a time series from distant earthquakes can often be removed from a time series without impacting the estimate of steady velocity, just as offsets in time series from equipment changes may be removed, and sometimes the same can be done for slow slip events. If the slip is known or estimated, and displacements are removed from the time series of positions, then the velocities computed from these corrected time series can be used to study steady motions. However, estimation of the slip in this way presumes that a 'steady' velocity can be defined, which is not always simple when multiple time-dependent events are occurring simultaneously. McCaffrey[66] addressed this problem by estimating a time-dependent deformation model combining steady and transient sources directly from the GPS time series.

Postseismic deformation

Because of the stress changes associated with large earthquakes, the pattern and rate of strain around a fault are often different immediately after an earthquake compared to the pre-earthquake time period. Postseismic deformation is the general term for the transient changes in deformation that follow earthquakes. The time dependence of postseismic deformation depends on the rheology of the crust and upper mantle[67] and it provides an opportunity to study the forces that drive tectonic deformation and the rheology of the crust and upper mantle. Postseismic deformation can be large and long lasting[68], although there is great variation from earthquake to earthquake. For example, postseismic deformation following the 1964 Alaska earthquake causes surface motions of as much as 15–20 mm/yr even 45 years after the earthquake[69]. Thus care needs to be taken to evaluate the potential impact of postseismic deformation on any deforming zone. The effects of postseismic deformation, if not modeled and removed, can significantly bias estimates of plate boundary deformation. Postseismic deformation makes it particularly important to include data from different times in the earthquake cycle, so that the non-elastic effects will be quite different in the different time periods. In practice, this will usually mean combining velocities from the period immediately before the earthquake with postseismic data. Such a data combination, where the earthquake history is well known, can allow estimation of both the long-term slip rate and the viscosity structure[70]. Hilley *et al.*[71] used a 3D viscoelastic model to explore the tradeoffs between long-term slip rate, rheological structure, and earthquake history in predicting observed present-day crustal deformation. Uncertainties in the rheology and earthquake history mean that the range of possible slip rates consistent with the deformation data is broader than would be estimated based on a purely elastic model.

Postseismic deformation results from a superposition of three main physical mechanisms: viscoelastic relaxation of the mantle and possibly lower crust, afterslip on the very shallow or deep parts of the fault zone, and poroelastic relaxation. Poroelastic relaxation, which is deformation driven by fluid flow that relieves pressure differences caused by the earthquake, is generally important only very close to the fault and near geometric complexities such as fault stepovers and bends. Shallow afterslip is a frictional process, first observed after the 1966 Parkfield earthquakes[72], that has been

observed after many subsequent earthquakes, including subduction zone events[73,74]. Deep afterslip may be a frictional process, a ductile shear process, or some combination of the two, and it is generally found immediately downdip of the coseismic rupture zone.

Our ability to measure steady rigid plate motions that are very close to long-term geological plate motion estimates places some useful constraints on the spatial and temporal extent of postseismic deformation, as do the many case studies now available. Some degree of localization of strain in the mantle beneath faults is required to recover steady plate motions in the plate interiors. Postseismic models in which the mantle is linear viscoelastic[75] predict transient deformations that always extend a great distance away from every active fault, even a long time after the last major earthquake. This is counter to observations made near the edges of the plate interiors, which agree with or are very close to geologic plate estimates. It is also counter to observations from a number of fault systems prior to large earthquakes, which show localized strain around the fault that matches the pattern of simple elastic dislocation models. The North Anatolian Fault in Turkey provides the strongest observational test, because GPS and InSAR data are available across several segments of the fault with varying time since the last earthquake, and both pre- and post-seismic data are available for the Izmit and Düzce segments of the fault. Hearn *et al.*[76] concluded that a linear (Maxwell) viscoelastic model cannot fit the postseismic data while remaining consistent with the localized interseismic deformation observed prior to the earthquake, and that the effective viscosity of the relaxing material (lower crust or upper mantle) must increase with time after large earthquakes. Data before and after the 2002 Denali Fault earthquake leads to a similar conclusion[61,77,78]. More than one type of nonlinear viscosity might satisfy these observations. Freed *et al.*[77] argued for a power-law viscosity, whereas Hearn *et al.*[76] preferred a Burger's body (transient) viscosity. Alternately, localization of strain could reflect lateral variations in material properties; this is more likely to be important for viscoelastic relaxation within the lithosphere than in the asthenosphere or below because of long-term motion of the lithosphere relative to the asthenosphere. The observed localization of deformation during the interseismic period makes it likely that the long-term fault motion rate and background deformation rate represent a balance between tectonic forces and the effective viscosity as measured over long time scales.

Although some progress has been made in the theoretical models, a convincing and complete model for the earthquake cycle that incorporates postseismic and interseismic deformation and agrees with data has not yet been developed. This probably will remain a focus of research for some time.

Changes in fault slip rates over time

In many cases, geologically estimated slip rates from dated fault offsets and geodetic slip rate estimates are in good agreement, but there are some significant disagreements that might imply changes in fault slip rates over time[79,80]. Thatcher[58] discussed this problem and highlighted the need for a critical examination of slip rate estimates from both sources before a definitive change in slip rate can be established.

For many years, there has been controversy over geologic and geodetic fault slip rates for some of the major faults in Asia, especially for the Altyn Tagh fault. Early studies of dated offsets of terrace risers estimated slip rates as high as 30 mm/yr (refs 81, 82), whereas geodetic data across the fault suggested a low slip rate, on the order of 10 mm/yr (refs 83, 84). Cowgill[85] argued that uncertainties in geologic estimates of slip rates based on offsets of terrace risers had been underestimated and that most published slip geological rate estimates for the Altyn Tagh fault actually represented upper bounds on the slip rate. Re-estimation of the slip rate at two locations, including both new data and estimates of the upper and lower bounds on terrace tread ages, gives a slip rate of 9–15 mm/yr, consistent with the geodetic estimates[86,87]. Zhang *et al.*[88] had previously reinterpreted dates of terrace risers and showed that age dates consistent with GPS rates were also consistent with geomorphic field relations.

One of the best examples of a possibly significant change in slip rate with time involves the Garlock Fault and Eastern California Shear Zone in the Mojave Desert of California. The Garlock fault is a left-lateral strike-slip fault that is in a conjugate orientation to the right-lateral San Andreas Fault and the faults of the Eastern California Shear zone. The present geodetic slip rate estimated for the Garlock fault[17] is significantly lower than expected based on the recent geological slip rate[89], whereas the reverse is true for the adjacent Eastern California Shear Zone[80,90]. Dolan *et al.*[91] and Oskin *et al.*[80] suggested that time-dependent behaviour of ductile shear zones in the deep crust may result in time-dependent fault slip, which in this case might result in switching between two modes: elevated slip rate on the Eastern California Shear Zone with low slip on the Garlock fault (the present) and elevated slip on the Garlock fault with low slip on the Eastern California Shear Zone (much of the geologically recent past). Alternately, the geodetic estimates might be biased by postseismic deformation from the Landers and Hector Mine earthquake or from past earthquakes on the San Andreas Fault[70]. All of the published geodetic rates are based on geodetic velocities from the SCEC crustal motion map, and postseismic deformation was not removed from the velocities in that product, although efforts were made to minimise its effects. Exploring this possibility will require analysis and modeling of long

post-earthquake time series and careful inclusion of the limited pre-earthquake data from the region.

Summary

The classic model of rigid plate tectonics explains the most important active tectonic features on Earth, but the assumption of plate rigidity breaks down in continental plate boundary zones. The plate boundary zones of Asia and western North America have been studied extensively and illustrate the typical features of plate boundary zones. In both plate boundary zones, crustal motions observed by geodesy can be described well by models that use a number of rigid plates or blocks, bounded by faults that are presumed to cut the entire lithosphere. Only a few areas, mostly in the Tibetan Plateau, may be exceptions to this rule. This might indicate that deformation in these regions is distributed at depth, even if it is localized at the surface. The size of the blocks needed to describe deformation with a plate/block model sometimes must be very small, with some lateral dimension smaller than the lithospheric thickness. Examples of this include the long, sliver-like blocks that are bounded by the major strand of the San Andreas Fault system in California. At a small enough spatial scale, the rigid block model becomes difficult to distinguish from distributed deformation.

The lithosphere of much East and Northeast Asia is fragmented into several rigid or very slowly straining regions, most likely small plates within the plate boundary zone. South China moves 8–10 mm/yr relative to the Eurasian plate, but relative motions of the Amurian and Okhotsk plates are substantially slower and the slow rate of motion makes it difficult to distinguish between a rigid plate and a region of slow, diffuse deformation. Thus, locations of plate boundaries and the existence of certain plates have been debated and models for the region are likely to be subject to future revisions. As in Asia, the western part of North America is fragmented into a large number of blocks or plates. The northwest limit of the stable North American plate is not clearly defined, but most likely the North American plate does not extend far beyond the Canadian arctic. Most of Alaska and the Northern Cordillera of Canada move relative to North America, the Bering Sea region forms a rigid Bering plate, and NE Siberia (Chukotka) and the arctic coast of Alaska show slow movement relative to North America that might represent motion of a rigid plate. In the latter case, slow, diffuse deformation and/or errors in the definition of the motion of North America in geodetic reference frames might also explain the observed velocities.

The plate boundary zones of Asia and North America are connected as part of a broad band of distributed deformation that marks the entire northern Pacific Rim. Combining the observations from Asia and North America, we find that the distributed deformation spans not only the India – Eurasia plate boundary zone, but also the Eurasia – North America plate boundary zone. Although some early work suggested that even the northern part of Japan might lie on the North American plate, a collage of smaller plates provides a better explanation. In fact, distributed deformation is continuous or nearly so from Baja California around the north Pacific to Tibet and beyond. Pervasive fragmentation of continental lithosphere at plate boundaries is the rule, not the exception.

Study of plate boundary zones is complicated by temporal variations in deformation, especially close to faults. Estimates of steady tectonic motion can be biased if temporal variations in slip (like earthquakes or slow slip events) or postseismic deformation are not correctly accounted for. Despite the time dependence implied by postseismic deformation data and models, the concept of an interseismic period dominated by steady deformation with time appears to remain valid. Observations of steady deformation localized around faults in the years before earthquakes and the ability to measure steady plate motions in agreement with geological rates, combined with observations of rapid postseismic deformation following earthquakes appear to require spatial viscosity variations or nonlinear viscoelasticity in the upper mantle; models that rely on uniform linear viscoelasticity for the mantle predict deformation far from the fault late in the earthquake cycle that is contrary to observations. The development of an earthquake cycle model that explains both pre- and post-earthquake observations remains an area of active research, although recent progress has been made. In addition, there is some evidence for changes in fault slip rates over time, particularly when pairs of faults within a small area show coupled behaviour. Although both geological and geodetic evidence for slip rate changes needs to be examined critically, there are a few examples where the evidence for changes in rate over a few thousand years appears to be persuasive.

1. DeMets, C., Gordon, R. G. and Argus, D. F., Geologically current plate motions. *Geophys. J. Int.*, 2010, **181**, 1–80; doi:10.1111/j.1365-246X.2009.04491.x.
2. Argus, D. F. *et al.*, The angular velocities of the plates and the velocity of Earth's centre from space geodesy. *Geophys. J. Int.*, 2010, **181**, 1–48; doi:10.1111/j.1365-246X.2009.04463.x.
3. Bird, P., An updated digital model of plate boundaries. *Geochem. Geophys. Geosyst.*, 2003, **4**(3), 1027; doi:10.1029/2001GC000252.
4. McCaffrey, R. *et al.*, Fault locking, block rotation and crustal deformation in the Pacific Northwest. *Geophys. J. Int.*, 2007, **169**, 1315–1340; doi:10.1111/j.1365-246X.2007.03371.x.
5. Sella, G. F., Dixon, T. H. and Mao, A., REVEL: a model for recent plate velocities from space geodesy. *J. Geophys. Res.*, 2002, **107**, 2081; doi:10.1029/2000JB000033.
6. Altamimi, Z., Collilieux, X., Legrand, J., Garayt, B. and Boucher, C., ITRF2005: a new release of International Terrestrial Reference Frame based on time series of station positions and Earth Orientation Parameters. *J. Geophys. Res.*, 2007, **112**, B004949; doi:10.1029/2007JB004949.

7. Norabuena, E. O., Dixon, T. H., Stein, S. and Harrison, C. G. A., Decelerating Nazca–South America and Nazca–Pacific Plate motions. *Geophys. Res. Lett.*, 1999, **26**, 3405–3408.
8. Calais, E., Han, J. Y., DeMets, C. and Nocquet, J. M., Deformation of the North American plate interior from a decade of continuous GPS measurements. *J. Geophys. Res.*, 2006a, **111**, B06402; doi:10.1029/2005JB004253.
9. Sella, G. F., Stein, S., Dixon, T. H., Craymer, M., James, T. S., Mazzotti, S. and Dokka, R. K., Observation of glacial isostatic adjustment in 'stable' North America with GPS. *Geophys. Res. Lett.*, 2007, **34**, L02306; doi:10.1029/2006GL027081.
10. Banerjee, P., Bürgmann, R., Nagarajan, B. and Apel, E., Intraplate deformation of the Indian subcontinent. *Geophys. Res. Lett.*, 2008, **35**, L18301; doi:10.1029/2008GL035468.
11. Scholz, C., *The Mechanics of Earthquakes and Faulting*, Cambridge University Press, Cambridge, 1990.
12. Reid, H. F., The elastic rebound theory of earthquakes. *Bull. Dept, Geol., Univ. Calif. Publ.*, 1911, **6**(19), 413–444.
13. Savage, J. C. and Burford, R. O., Accumulation of tectonic strain in California. *Bull. Seismol. Soc. Am.*, 1970, **60**, 1877–1896.
14. Savage, J., A dislocation model of strain accumulation and release at a subduction zone. *J. Geophys. Res.*, 1983, **88**, 4984–4996.
15. McCaffrey, R., Crustal block rotations and plate coupling. In *Plate Boundary Zones* (eds Stein, S. and Freymueller, J.), AGU Geodynamics Series 30, 2002, pp. 101–122.
16. Meade, B. J. and Hager, B. H., Block models of crustal motion in southern California constrained by GPS measurements. *J. Geophys. Res.*, 2005a, **110**, B03403; doi:10.1029/2004JB003209.
17. Meade, B. J. and Hager, B. H., Spatial localization of moment deficits in southern California. *J. Geophys. Res.*, 2005b, **110**, B04402; doi:10.1029/2004JB003331.
18. Nyst, M. and Thatcher, W., New constraints on the active tectonic deformation of the Aegean. *J. Geophys. Res.*, 2004, **109**, B11406; doi:10.1029/2003JB002830.
19. Reilinger, R. *et al.*, GPS constraints on continental deformation in the Africa–Arabia–Eurasia continental collision zone and implications for the dynamics of plate interactions. *J. Geophys. Res.*, 2006, **111**, B05411; doi:10.1029/2005JB004051.
20. Meade, B. J., Present-day kinematics at the India–Asia collision zone. *Geology*, 2007, **35**, 81–84; doi:10.1130/G22924A.1.
21. Loveless, J. P. and Meade, B. J., Geodetic imaging of plate motions, slip rates, and partitioning of deformation in Japan. *J. Geophys. Res.*, 2010, **115**, B02410; doi:10.1029/2008JB006248.
22. Freymueller, J. T., Murray, M. H., Segall, P. and Castillo, D., Kinematics of the Pacific–North America plate boundary zone, Northern California. *J. Geophys. Res.*, 1999, **104**, 7419–7441.
23. Haines, A. J. and Holt, W. E., A procedure to obtain the complete horizontal motions within zones of distributed deformation from the inversion of strain rate data. *J. Geophys. Res.*, 1993, **98**, 12057–12082.
24. Flesch, L. M., Haines, A. J. and Holt, W. E., Dynamics of the India–Eurasia collision zone. *J. Geophys. Res.*, 2001, **106**(B8), 16435–16460.
25. Flesch, L. M., William, E. H., Haines, A. J., Wen, L. and Shen-Tu, B., The dynamics of western North America: stress magnitudes and the relative role of gravitational potential energy, plate interaction at the boundary and basal tractions. *Geophys. J. Int.*, 2007, **169**(3), 866; doi:10.1111/j.1365-246X.2007.03274.x.
26. Gordon, D., Ma, C. and Ryan, J. W., Results from the CDP mobile VLBI program in the western United States. In *Contributions of Space Geodesy to Geodynamics: Crustal Dynamics* (eds Smith, D. E. and Turcotte, D. L.), AGU Geophysical Monograph, 23, American Geophysical Union, Washington, 1993, pp. 131–138.
27. McCaffrey, R., Block kinematics of the Pacific–North America plate boundary in the southwestern US from inversion of GPS, seismological, and geologic data. *J. Geophys. Res.*, 2005, **110**, B07401; doi:10.1029/2004JB003307.
28. Payne, S. J., McCaffrey, R. and King, R. W., Strain rates and contemporary deformation in the Snake River Plain and surrounding Basin and Range from GPS and seismicity. *Geology*, 2008, **36**, 647–650.
29. Puskas, C. M. and Smith, R. B., Intraplate deformation and microplate tectonics of the Yellowstone hot spot and surrounding western US interior. *J. Geophys. Res.*, 2009, **114**, B04410; doi:10.1029/2008JB005940.
30. Lahr, J. C. and Plafker, G., Holocene Pacific–North American Plate interaction in southern Alaska; implications for the Yakataga seismic gap. *Geology*, 1980, **8**, 483–486.
31. Fletcher, H. J., Crustal deformation in Alaska measured using the Global Positioning Systeml, Ph D thesis, University of Alaska Fairbanks, 2002, pp. 135.
32. Mazzotti, S. and Hyndman, R., Yakutat collision and strain transfer across the northern Canadian Cordillera. *Geology*, 2002, **30**, 495–498.
33. Oldow, J. S., Bally, A. W. and Ave Lallemant, H. G., Transpression, orogenic float, and lithospheric balance. *Geology*, 1990, **18**, 991–994.
34. Leonard, L. J., Hyndman, R. D., Mazzotti, S., Nykolaishen, L., Schmidt, M. and Hippchen, S., Current deformation in the northern Canadian Cordillera inferred from GPS measurements. *J. Geophys. Res.*, 2007, **112**, B11401; doi:10.1029/2007JB005061.
35. Leonard, L. J., Mazzotti, S. and Hyndman, R. D., Deformation rates estimated from earthquakes in the northern Cordillera of Canada and eastern Alaska. *J. Geophys. Res.*, 2008, **113**, B08406; doi:10.1029/2007JB005456.
36. Mazzotti, S., Leonard, L. J., Hyndman, R. D. and Cassidy, J. F., Tectonics, dynamics, and seismic hazard in the Canada–Alaska Cordillera. In *Active Tectonics and Seismic Potential of Alaska*, American Geophysical Union Geophysical Monograph no. 179, 2008, pp. 297–319.
37. Elliott, J., Larsen, C. F., Freymueller, J. T. and Motyka, R. J., Tectonic block motion and glacial isostatic adjustment in Southeast Alaska and adjacent Canada constrained by GPS measurements. *J. Geophys. Res.*, 2010; doi:10.1029/2009JB007139.
38. Mazzotti, S., Hyndman, R. D., Flück, P., Smith, A. J. and Schmidt, M., Distribution of the Pacific/North America motion in the Queen Charlotte Islands – S. Alaska plate boundary zone. *Geophys. Res. Lett.*, 2003, **30**, 1762; doi:10.129/2003GL017586.
39. Cross, R. S. and Freymueller, J. T., Evidence for and implications of a Bering plate based on geodetic measurements from the Aleutians and western Alaska. *J. Geophys. Res.*, 2008, **113**, B07405; doi:10.1029/2007JB005136.
40. Avouac, J. and Tapponnier, P., Kinematic model of active deformation in central Asia. *Geophys. Res. Lett.*, 1993, **20**, 895–898; doi:10.1029/93GL00128.
41. England, P. and McKenzie, D., A thin viscous sheet model for continental deformation. *Geophys. J. R. Astron. Soc.*, 1982, **70**, 295–321.
42. Replumaz, A. and Tapponnier, P., Reconstruction of the deformed collision zone between India and Asia by backward motion of lithospheric blocks. *J. Geophys. Res.*, 2003, **108**, 2285; doi:10.1029/2001JB000661.
43. Shen, Z.-K., Zhao, C., Yin, A., Li, Y., Jackson, D. D., Fang, P. and Dong, D., Contemporary crustal deformation in east Asia constrained by Global Positioning System measurements. *J. Geophys. Res.*, 2000, **105**(B3), 5721–5734.
44. Shen, Z.-K., Lü, J., Wang, M. and Bürgmann, R., Contemporary crustal deformation around the southeast borderland of the Tibetan Plateau. *J. Geophys. Res.*, 2005, **110**, B11409; doi:10.1029/2004JB003421.
45. Chen, Q., Freymueller, J., Wang, Q., Yang, Z., Xu, C. and Liu, J., A deforming block model for the present-day tectonics of Tibet. *J. Geophys. Res.*, 2004, **109**(B1), B01403; doi:10.1029/2002JB002151.

46. Wang, Q. *et al.*, Present-day crustal deformation in China constrained by Global Positioning System measurements. *Science*, 2001, **294**, 574–577.
47. Zhang, P.-Z. *et al.*, Continuous deformation of the Tibetan Plateau from Global Positioning System data. *Geology*, 2004, **32**, 809–812; doi:10.1130/G20554.1.
48. Gan, W. *et al.*, Present day crustal motion within the Tibetan Plateau inferred from GPS measurements. *J. Geophys. Res.*, 2007, **112**, B08416; doi:10.1029/2005JB004120.
49. Thatcher, W., Microplate model for the present-day deformation of Tibet. *J. Geophys. Res.*, 2007, **112**, B01401; doi:10.1029/2005JB004244.
50. Calais, E., Vergnolle, M., San'kov, V., Lukhnev, A., Miroshnitchenko, A., Amarjargal, S. and Dverchre, J., GPS measurements of crustal deformation in the Baikal-Mongolia area (1994–2002): implications for current kinematics of Asia. *J. Geophys. Res.*, 2003, **108**(B10), 2501; doi:10.1029/2002JB002373.
51. Heki, K. *et al.*, The Amurian Plate motion and current plate kinematics in eastern Asia. *J. Geophys. Res.*, 1999, **104**(B12), 29147–29155.
52. Cook, D. B., Fujita, K. and McMullen, C. A., Present-day plate interactions in northeast Asia–North-American, Eurasian, and Okhotsk plates. *J. Geodyn.*, 1986, **6**, 33–51.
53. Riegel, S. A., Fujita, K., Kozmin, B. M., Imaev, V. S. and Cook, D. B., Extrusion tectonics of the Okhotsk Plate, northeast Asia. *Geophys. Res. Lett.*, 1993, **20**(7), 607–610.
54. Apel, E. V., Bürgmann, R., Steblov, G., Vasilenko, N., King, R. and Prytkov, A., Independent active microplate tectonics of northeast Asia from GPS velocities and block modeling. *Geophys. Res. Lett.*, 2006, **33**, L11303; doi:10.1029/2006GL026077.
55. Calais, E., Dong, L., Wang, M., Shen, Z. and Vergnolle, M., Continental deformation in Asia from a combined GPS solution. *Geophys. Res. Lett.*, 2006b, **33**, L24319; doi:10.1029/2006GL028433.
56. Vergnolle, M., Calais, E. and Dong, L., Dynamics of continental deformation in Asia. *J. Geophys. Res.*, 2007, **112**, B11403; doi:10.1029/2006JB004807.
57. Stein, S., Space geodesy and plate motions. In *Contributions of Space Geodesy to Geodynamics: Crustal Dynamics* (eds Smith, D. E. and Turcotte, D. L.), AGU Geophysical Monograph 23, American Geophysical Union, Washington, 1993, pp. 5–20.
58. Thatcher, W., How the continents deform: the evidence from tectonic geodesy. *Ann. Rev. Earth Planet. Sci.*, 2009, **37**, 237–262; doi:10.1146/annurev.earth.031208.100035.
59. Bourne, S. J., England, P. C. and Parsons, B., The motion of crustal blocks driven by flow of the lower lithosphere and implications for slip rates of continental strike-slip faults. *Nature*, 1998, **391**, 655–659.
60. Thatcher, W., GPS constraints on the kinematics of continental deformation. *Int. Geol. Rev.*, 2003, **45**, 191–212.
61. Freymueller, J. T. *et al.*, Active deformation processes in Alaska, based on 15 years of GPS measurements. In *Active Tectonics and Seismic Potential of Alaska* (eds Freymueller, J. T. *et al.*), AGU Geophysical Monograph 179, AGU, Washington, DC, 2008, pp. 1–42.
62. Liu, Z. and Bird, P., Kinematic modelling of neotectonics in the Persia–Tibet–Burma orogen. *Geophys. J. Int.*, 2008, **172**, 779–797; doi:10.1111/j.1365-246X.2007.03640.x.
63. Kogan, M. G. and Steblov, G. M., Current global plate kinematics from GPS (1995–2007) with the plate-consistent reference frame. *J. Geophys. Res.*, 2008, **113**, B04416; doi:10.1029/2007JB005353.
64. Rogers, G. and Dragert, H., Episodic tremor and slip on the Cascadia subduction zone: the chatter of silent slip. *Science*, 2003, **300**, 1942–1943; doi:10.1126/science.1084783.
65. Schwartz, S. Y. and Rokosky, J. M., Slow slip events and seismic tremor at circum-Pacific subduction zones. *Rev. Geophys.*, 2007, **45**, RG3004; doi:10.1029/2006RG000208.
66. McCaffrey, R., Time-dependent inversion of three-component continuous GPS for steady and transient sources in northern Cascadia. *Geophys. Res. Lett.*, 2009, **36**, L07304; doi:10.1029/2008GL036784.
67. Bürgmann, R. and Dresen, G., Rheology of the lower crust and upper mantle: evidence from rock mechanics, geodesy and field observations. *Ann. Rev. Earth Planet. Sci.*, 2008, **36**, 531–567; doi:10.1146/annurev.earth.36.031207.124326.
68. Wang, K., Elastic and viscoelastic models of crustal deformation in subduction earthquake cycles. In *The Seismogenic Zone of Subduction Thrust Faults* (eds Dixon, T. H. and Moore, J. C.), Columbia Univ. Press, New York, 2007, pp. 540–575.
69. Suito, H. and Freymueller, J. T., A viscoelastic and afterslip postseismic deformation model for the 1964 Alaska earthquake. *J. Geophys. Res.*, 2009, **114**, B11404; doi:10.1029/2008JB005954.
70. Johnson, K. M., Hilley, G. E. and Bürgmann, R., Influence of lithosphere viscosity structure on estimates of fault slip rate in the Mojave region of the San Andreas fault system. *J. Geophys. Res.*, 2007, **112**, B07408; doi:10.1029/2006JB004842.
71. Hilley, G. E., Johnson, K. M., Wang, M., Shen, Z.–K. and Bürgmann, R., Earthquake-cycle deformation and faultslip rates in northern Tibet. *Geology*, 2009, **37**, 31–34; doi:10.1130/G25157A.1.
72. Smith, S. W. and Wyss, M., Displacement on the San Andreas fault subsequent to the 1966 Parkfield earthquake. *Bull. Seismol. Soc. Am.*, 1968, **58**, 1955–1973.
73. Hsu, Y. J. *et al.*, Frictional afterslip following the 2005 Nias-Simeulue earthquake, Sumatra. *Science*, 2006, **312**, 1921–1926; doi:10.1126/science.1126960.
74. Kreemer, C., Blewitt, G. and Maerten, F., Co- and postseismic deformation of the 28 March 2005 Nias M_w 8.7 earthquake from continuous GPS data. *Geophys. Res. Lett.*, 2006, **33**, L07307; doi:10.1029/2005GL025566.
75. Savage, J. and Prescott, W., Asthenosphere readjustment and the earthquake cycle. *J. Geophys. Res.*, 1978, **83**, 3369–3376.
76. Hearn, E. H., McClusky, S., Ergintav, S. and Reilinger, R. E., Izmit earthquake postseismic deformation and dynamics of the North Anatolian Fault Zone. *J. Geophys. Res.*, 2009, **114**, B08405; doi:10.1029/2008JB006026.
77. Freed, A., Bürgmann, R., Calais, E. and Freymueller, J., Stress-dependent power-law flow in the upper mantle following the 2002 Denali, Alaska, earthquake. *EPSL*, 2006, **252**, 481–489.
78. Freymueller, J. T., Freed, A. M., Johnson, K. M., Bürgmann, R., Calais, E., Pollitz, F. F. and Biggs, J., Denali fault earthquake postseismic deformation models. *Eos Trans. AGU*, 2009, **90**(52), Fall Meet. Suppl., Abstract G34A-05.
79. Bennett, R. A., Friedrich, A. M. and Furlong, K. P., Codependent histories of the San Andreas and San Jacinto fault zones from inversion of fault displacement rates. *Geology*, 2004, **32**, 961–964.
80. Oskin, M., Perg, L., Shelef, E., Strane, M., Gurney, E., Singer, B. and Zhang, X., Elevated shear zone loading rate during an earthquake cluster in eastern California. *Geology*, 2008, **36**, 507–510; doi:10.1130/G24814A.1.
81. Peltzer, G., Tapponnier, P. and Armijo, R., Magnitude of the Quaternary left-lateral displacements along the north edge of Tibet. *Science*, 1989, **246**, 1285–1289.
82. Mériaux, A.-S. *et al.*, Rapid slip along the central Altyn Tagh Fault: Morphochronologic evidence from Cherchen He and Sulamu Tagh. *J. Geophys. Res.*, 2004, **109**, B06401; doi:10.1029/2003JB002558.
83. Bendick, R., Bilham, R., Freymueller, J., Larson, K. and Yin, G., Geodetic evidence for a low slip rate in the Altyn Tagh fault and constraints on the deformation of Asia. *Nature*, 2000, **404**, 69–72.
84. Wallace, K., Yin, G. and Bilham, R., Inescapable slow slip on the Altyn Tagh fault. *Geophys. Res. Lett.*, 2004, **31**, L09613; doi:10.1029/2004GL019724.

85. Cowgill, E., Impact of riser reconstructions on estimation of secular variation in rates of strike-slip faulting: revisiting the Cherchen River site along the Altyn Tagh fault, NW China. *Earth Planet. Sci. Lett.*, 2007, **254**, 239–255.
86. Cowgill, E., Gold, R., Xuanhua, C., Xiaofeng, W., Arrowsmith, J. R. and Southon, J. R., Resolving the slip-rate discrepancy along the longest active strike-slip fault in Tibet. *Geology*, 2009, **37**(7), 647–650; doi:10.1130/G25623A.1.
87. Gold, R. D., Cowgill, E., Arrowsmith, J. R., Gosse, J., Chen, X. and Wang, X., Riser diachroneity, lateral erosion, and uncertainty in rates of strike-slip faulting: a case study from Tuzidun along the Altyn Tagh Fault, NW China. *J. Geophys. Res.*, 2009, **114**, B04401; doi:10.1029/2008JB005913.
88. Zhang, P.-Z., Molnar, P. and Xu, X., Late Quaternary and present-day rates of slip along the Altyn Tagh Fault, northern margin of the Tibetan Plateau. *Tectonics*, 2007, **26**, TC5010; doi:10.1029/2006TC002014.
89. McGill, S. F., Wells, S. G., Fortner, S. K., Kuzma, H. A. and McGill, J. D., Slip rate of the western Garlock fault, at Clark Wash, near Lone Tree Canyon, Mojave Desert, California. *Geol. Soc. Am. Bull.*, 2009, **121**, 536–554; doi:10.1130/B26123.1.
90. Peltzer, G., Crampe, F., Hensley, S. and Rosen, P., Transient strain accumulation and fault interaction in the eastern California shear zone. *Geology*, 2001, **29**, 975–978.
91. Dolan, J. F., Bowman, D. D. and Sammis, C. G., Long range and long-term fault interactions in Southern California. *Geology*, 2007, **35**, 855–858; doi:10.1130/G23789A.1.
92. Wessel, P. and Smith, W. H. F., Free software helps map and display data. *Eos Trans. AGU*, 1991, **72**, 441.
93. Apel, E. V., Bürgmann, R. and Banerjee, P., India plate motion, deformation, and plate boundary interaction. *Geophys. J. Int.* (submitted).
94. Taylor, M. and Yin, A., Active structures of the Himalayan–Tibetan orogen and their relationships to earthquake distribution, contemporary strain field, and Cenozoic volcanism. *Geosphere*, 2009, **5**, 199–214.
95. Styron, R., Taylor, M. and Okoronkwo, K., Database of active structures from the Indo-Asian collision. *Eos Trans. AGU*, 2010, 91(20); doi:10.1029/2010EO200001.

ACKNOWLEDGEMENTS. I thank Roland Bürgmann, John Paul Puchakayala and Julie Elliott for helpful reviews of the manuscript, and Trey Apel for providing plate outlines from his submitted paper. Financial support has been provided by several grants from the US National Science Foundation, including EAR-0408799. The maps were created using the GMT software[92].